

Chitosan-mediated *in situ* biomolecule assembly in completely packaged microfluidic devices

Jung Jin Park,^{ab} Xiaolong Luo,^{ac} Hyunmin Yi,^{†b} Theresa M. Valentine,^{‡ab} Gregory F. Payne,^{ce} William E. Bentley,^{ce} Reza Ghodssi^{acd} and Gary W. Rubloff^{*abcf}

Received 1st March 2006, Accepted 4th July 2006

First published as an Advance Article on the web 27th July 2006

DOI: 10.1039/b603101c

We report facile *in situ* biomolecule assembly at readily addressable sites in microfluidic channels after complete fabrication and packaging of the microfluidic device. Aminopolysaccharide chitosan's pH responsive and chemically reactive properties allow electric signal-guided biomolecule assembly onto conductive inorganic surfaces from the aqueous environment, preserving the activity of the biomolecules. A transparent and nonpermanently packaged device allows consistently leak-free sealing, simple *in situ* and *ex situ* examination of the assembly procedures, fluidic input/outputs for transport of aqueous solutions, and electrical ports to guide the assembly onto the patterned gold electrode sites within the channel. Both *in situ* fluorescence and *ex situ* profilometer results confirm chitosan-mediated *in situ* biomolecule assembly, demonstrating a simple approach to direct the assembly of biological components into a completely fabricated device. We believe that this strategy holds significant potential as a simple and generic biomolecule assembly approach for future applications in complex biomolecular or biosensing analyses as well as in sophisticated microfluidic networks as anticipated for future lab-on-a-chip devices.

Introduction

Microfluidic devices have recently gained significant attention due to their broad applications for biosensors,^{1–4} biomedical synthesis/analysis applications,^{5–8} and metabolic engineering.⁹ Recent advances in fabrication techniques significantly scaled down the dimensions allowing smaller sample sizes and high throughput screening capabilities for various analytical procedures such as capillary electrophoresis, polymerase chain reaction and drug screening.^{1,10–12} Despite such advances, assembling biological components in the microfluidic devices in their active forms with spatial selectivity still remains challenging.

Conventional methods to add biological components to devices include optical methods such as photolithography, mechanical methods such as ink jet printing, soft lithography and microcontact printing, involving chemical reactions at

various stages.^{13–17} While these methods are being rapidly developed and widely adapted, each method encounters limitations such as arduous chemical procedures, requirements for complicated robotic facilities, dry environment and lack of flexibility that may destroy activities of the biomolecules being assembled. It is thus highly desirable that the biomolecule assembly step be performed *in situ* from the aqueous environment after complete fabrication and packaging of the device.

We have been exploiting biopolymer chitosan as the biomolecule assembly scaffold to achieve such a goal.¹⁸ Chitosan is an aminopolysaccharide with unique properties that can be harnessed to assemble biological molecules onto conductive surfaces. As shown in Fig. 1(a), each glucosamine monomer unit of chitosan has a primary amine group with a low pK_a value (≈ 6.3), which is protonated and positively charged at low pH, making chitosan soluble in aqueous solution. At neutral to high pH, this amine group becomes deprotonated and uncharged, thus making chitosan insoluble biopolymeric hydrogel networks. As shown in Fig. 1(b), this pH-responsive property allows assembly of chitosan from aqueous solution onto a negatively biased electrode surface due to the high local pH near the electrode in a highly spatially selective manner.^{19,20} Further, this primary amine group is nucleophilic at neutral state thus allowing various amine group reactive chemistries to be used for covalent conjugation of biomolecules onto chitosan.^{18,21,22} Combination of these two unique properties, namely pH-responsiveness and chemical reactivity, holds significant potential for post-fabrication biomolecule assembly in the microfluidic devices (Fig. 1(c)) since the assembly of the chitosan scaffold occurs in response to an electrical signal from the device to the aqueous solution, and the subsequent procedures for biomolecule conjugation

^aInstitute for Systems Research, University of Maryland, College Park, MD, 20742, USA

^bDepartment of Materials Science and Engineering, University of Maryland, College Park, MD, 20742, USA

^cBioengineering Graduate Program, University of Maryland, College Park, MD, 20742, USA

^dDepartment of Electrical and Computer Engineering, University of Maryland, College Park, MD, 20742, USA

^eCenter for Biosystems Research, University of Maryland Biotechnology Institute, College Park, MD, 20742, USA

^fInstitute for Research in Electronics and Applied Physics, University of Maryland, College Park, MD, 20742, USA. E-mail: rubloff@umd.edu; Fax: +1 301 314-9920; Tel: +1 301 405-2949

[†] Currently in the Department of Chemical and Biological Engineering, Tufts University, Medford, MA 02155, USA.

[‡] Currently in the US Nuclear Regulatory Commission, Washington, DC 20555, USA.

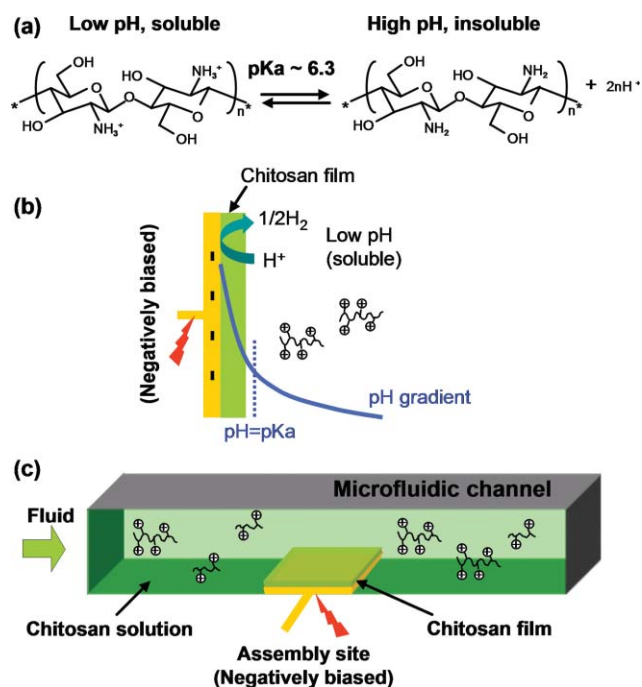


Fig. 1 (a) pH dependent protonation/deprotonation of the chitosan molecule; (b) schematic view of chitosan deposition; (c) schematic view of chitosan deposition in a microfluidic channel.

are also carried out in a closed aqueous environment avoiding drying, damaging or contamination.

In this paper, we report the development of a microfluidic system to achieve post-fabrication biomolecule assembly in the microfluidic environment. As shown in Fig. 2, our microfluidic device design employs microfabricated SU8 on a Pyrex wafer that defines the microfluidic channel structure, and patterned gold electrodes at the bottom of each microchannel as the readily addressable biomolecule assembly sites. Nonpermanent and leak-tight sealing of the microfluidic channels at the device level is then achieved by sealing the wafer with a PDMS-spun top sealing Plexiglas plate and then packaging with pressure-adjustable compression bolts (Fig. 3). Finally, fluidic and electric input/output ports are connected to microchannels for micropump-driven transport and electric signal-guided assembly of biomolecules from the aqueous environment.

Taking advantage of this microfluidic system we then demonstrate post-fabrication, *in situ* biomolecule assembly using the electrodeposition of chitosan at readily addressable assembly sites within the microfluidic channels. In this work, we first use fluorescently labeled chitosan to directly demonstrate biomolecule assembly at specific electrodes inside a microfluidic channel within the completely packaged microfluidic device, indicating the potential of this platform for biomolecular reaction processes. We then assemble fluorescent marker molecules, fluorescein and green fluorescent protein (GFP), onto an electrodeposited chitosan scaffold, illustrating electric signal-guided *in situ* biomolecule assembly at readily addressable sites in the microfluidic channels. These results demonstrate the first signal-directed chitosan-mediated biomolecule assembly in the microfluidic environment after complete packaging of the microfluidic device. We then

further examine the biopolymeric scaffold by *ex situ* profilometer measurements, illustrating the advantage of our nonpermanent sealing/packaging strategy. We believe that this post-fabrication, *in situ* biomolecule assembly strategy would be readily applicable to future microfluidic device designs that require approaches to simple multi-species biofunctionalization in three dimensional networks.^{23–25}

In particular, this work represents our ongoing efforts to harness microfabricated devices to actively engage biomolecular reactions, in this case by guiding spatially selective *in situ* biomolecule assembly through electric signals.

Materials and methods

Pyrex substrates for microfluidic device

There are several ways to create holes in the Pyrex wafer, such as wet/dry etching, laser drilling^{26–28} but these methods require long process times and are not cost effective. We adapted a simple drilling method to generate holes on the Pyrex wafer by using silica grit and brass tubing. Before drilling, both sides of the Pyrex wafer (4" diameter, 500 μm thick) were passivated with a photoresist (Shipley 1318) to prevent scratching and to minimize surface contamination during machining processes. Then the Pyrex wafer was fixed on a 1/2" thick Pyrex plate with a mounting media (Quick-StickTM, Cargille Labs) which is melted at 65 °C on a hot plate. After the cooling process at room temperature, 1/4" diameter holes for the compression bolts were drilled in the 4" Pyrex wafer using a brass tube and 30 μm size of silicon carbide grit (Universal photonics Inc.) in a milling machine. One hole in the center and 6 equally spaced holes around the edge of the wafer on a 1.75" radius were drilled. After drilling, the wafer and the plate were put on a hotplate at 65 °C to melt the mounting media and the wafer was removed from the thick Pyrex plate. Residue of wax and photoresist on the wafer was completely removed with acetone and by immersing in photoresist stripper at 65 °C for 10 min.

Gold electrode patterning and SU8 microchannel fabrication

The drilled 4" Pyrex wafer was cleaned with piranha solution ($\text{H}_2\text{SO}_4 : \text{H}_2\text{O}_2 = 3 : 1$, for 5 min) before electrode metal deposition. Thin layers of a Cr adhesion layer (90 Å) and then the Au electrode metal (2000 Å) were then deposited on the Pyrex wafer in a sputter deposition system. The wafer was cleaned with acetone, methanol and then finally isopropanol, and dehydrated at 100 °C for 10 min on a hot plate before electrode patterning. Photoresist was then spun onto the wafer and patterned with the electrode mask using contact photolithography.²⁹ After another cleaning process as described above, SU8-50 (MicroChem, Newton, MA) was spun on the wafer. To avoid the severe non-uniformity in SU8 film thickness which occurred near the drilled holes in the Pyrex wafer, we attached scotch tape on the backside of the drilled hole, filled the holes with SU8 solution using a pipette, and baked the structure for 60 min at 95 °C to harden the SU8 inside the drilled holes. Then an SU8 film was spun onto the Pyrex wafer using a spin speed of 1000 rpm for 15 s (achieving an SU8 thickness $\sim 150 \mu\text{m}$), which was followed by a soft baking process at 95 °C for 60 min. SU8 microchannels were

patterned using a transparency mask in a UV aligner (1000 mJ cm⁻², 405 nm UV line), followed by a post baking process at 95 °C for 30 min. Finally, the SU8 film was developed in SU8 developer (MicroChem) for 25 min. The thickness of SU8 film was measured by a mechanical profilometer (Dektak 6 M, Veeco Instruments Inc), which showed 10% thickness variation across the wafer.

Plexiglas package fabrication

The package which compresses the SU8–PDMS seal of the microfluidic system includes four Plexiglas plates—the top sealing plate which serves as the PDMS substrate analogous to the 4" Pyrex substrate for the SU8 microfluidic channels, two Plexiglas compression plates which push the top sealing plate and Pyrex substrate together to join the SU8/PDMS junction, and a Plexiglas I/O ring which carries fluidic and electrical connections from the package to external control systems. To package the 4" Pyrex substrate, the Plexiglas pieces were outfitted with through holes for compression bolts as well as fluidic I/O lines and electrical feedthroughs drilled at the assigned locations. After the machining process, a PDMS (Sylgard 184, Dow Corning) gasket film (~300 µm thick) was spun on a top sealing plate. A cork borer was used to punch holes in the PDMS film for fluidic and electrical feedthroughs because the PDMS film covers the drilled holes in the top sealing plate. The fluidic I/O's were made leak-tight using O-rings (Buna-N 004) inserted between top compression plate and top sealing plate, together with fluidic connectors (Nanoport[®]) bonded to the top compression plate with adhesives. Pogo pins (Interconnect Devices, Inc.) for electrical connection to the gold electrodes were inserted through the electrical feedthroughs. Socket head cap screws (¼"-28) and socket set screws (4-40) were used as compression bolts and force tunable screws respectively, with the latter provided to fine tune the stress distribution applied by the top compression plate to the top sealing plate to optimize SU8/PDMS sealing.

Electrodeposition of fluorescein labeled chitosan film

First, fluorescently labeled chitosan solution (0.5% w/v, pH ~ 5) was prepared for the deposition in a microfluidic system.²⁰ The chitosan solution was introduced through a tubing (0.19 mm ID, Tygon[®]) into the microfluidic system by a micropump (Masterflex[®] pump drive, Cole-Palmer Instrument Co) with a flow rate of 5 µl min⁻¹. After the microchannel with two electrodes at the channel bottom was completely filled with chitosan solution, the pump was stopped and a constant current signal of 2 A m⁻² by a power supply (Keithly 2400 source meter) was applied for 4 min to electrodeposit chitosan onto the negatively biased working electrode. LabView control software was used to control the chitosan electrodeposition process and to monitor the voltage of the applied electrical signal, which showed 2–3 V during the electrodeposition process. Then the pump was switched on again to drain chitosan solution and DI water was provided to rinse out excessive chitosan molecules loosely attached on the deposited chitosan film. For real-time, *in situ* fluorescence observation of the localized chitosan electrodeposition, the

microfluidic device was placed under a microscope (Zeiss model 310) equipped with a UV source (Zeiss HBO 100) equipped with a filter set matched to NHS-fluorescein (excitation band 490–495 nm, emission band 520–525 nm). Photomicrographs were prepared from the microscope using a digital camera (Carl Zeiss AxioCam MRc5).

Fluorescent labeling of electrodeposited chitosan film

To avoid cross contamination between the several solutions, we used multiple tubing for each solution and a LabView based fluidic control system was developed to enhance control over multiple solutions and processes. First, microchannel and tubing were cleaned with distilled water, HCl, and finally distilled water for 30 min, 5 min, and 30 min respectively, with flow rate of ~50 µl min⁻¹. The chitosan solution (0.375% (w/v), pH ~ 5) was introduced through a tubing (0.19 mm ID, Tygon[®]) into the microfluidic system by a micropump with a flow rate of 5 µl min⁻¹. With the pump stopped, chitosan film was deposited on the negatively biased electrode with current density of 3 A m⁻² for 240 s. Then the pump was switched on again to drain chitosan solution and phosphate buffered saline (PBS) buffer (pH ~ 7) was provided to neutralize the deposited chitosan film for 30 min with a 5 µl min⁻¹ flow rate. Then we introduced carboxyfluorescein succinimidyl ester (NHS-fluorescein) solution over the deposited chitosan film for 30 min with a 5 µl min⁻¹ flow rate. For real-time, *in situ* fluorescence observation and image acquisition of the fluorescent labeling of the electrodeposited chitosan film, the same optical microscopy set up was used as described above. Finally PBS buffer was provided to rinse the remaining NHS-fluorescein solution in the microchannel. To demonstrate negative control of this experiment, we repeated this experiment with the same process sequence but voltage was not applied. To analyze the 3-D contour and profile of fluorescent intensity from fluorescently labeled chitosan, we used ImageJ software (National Institutes of Health). Mechanical profilometer (Veeco, Dektak 6 M Stylus Profiler) was used to measure the thickness of the chitosan layer in the microchannel by opening the nonpermanently packaged device.

GFP assembly on electrodeposited chitosan film

We deposited unlabeled chitosan film inside the microchannel and green fluorescent protein (GFP) was assembled onto the chitosan film *via* glutaraldehyde crosslinking reagent. First, the same cleaning steps, chitosan deposition process, and PBS buffer neutralization steps were performed as described above. Glutaraldehyde solution (0.5%) was then introduced at 5 µl min⁻¹ for 30 min, followed by PBS buffer rinsing for 30 min. GFP solution was then flowed in the microfluidic channels for 15 min with a 5 µl min⁻¹ flow rate. For *in situ*, real time observation on the test site, the microfluidic system was placed under the microscope during the whole process. Finally, the microfluidic channel was rinsed with 5 µl min⁻¹ PBS for 30 min. For the negative control, we repeated the same processes on a separate channel of the microfluidic device, except that no voltage was applied to the electrode. ImageJ analysis software and mechanical profilometer were used to analyze fluorescent 3-D contour and internal bio-structure.

Results and discussion

Microfluidic device wafer design and fabrication

To develop a microfluidic device that enables electric signal-guided, post-fabrication biomolecule assembly in a spatially selective manner, we first designed simple networks of microchannels with patterned gold electrodes on a Pyrex wafer as shown in Fig. 2. Our microfluidic device has several features including all-transparent materials for simple *in situ* microscopic observation of biomolecule assembly events, nonpermanent sealing and packaging for further *ex situ* examination of the assembled biomolecules, and flexible PDMS-spun Plexiglas top sealing plate for consistently leak-free sealing. Fig. 2(a) shows the design of a microfluidic device wafer composed of 6 identical microchannels, gold electrodes and fluidic and electrical I/Os on a 4" Pyrex substrate. Drilled holes through the Pyrex are provided at the center and around the edge to allow compression system bolts to pass through. Also shown on the right side of Fig. 2(a) is a 3-D diagram of a gold electrode, the biomolecule assembly site, inside a microfluidic channel. Fig. 2(b) shows a close-up view of one of the fabricated microchannels. Fig. 2(c) shows a patterned gold electrode (1 mm × 1 mm) at the bottom of a microfluidic channel (500 μm wide), which serves as the electric signal-guided biomolecule assembly site. The SU8 microchannel pattern is restricted to a small lateral extent on either side of each microchannel. The SU8 pattern (400 μm wide, 150 μm deep) defines the channel structure to seal the channel by compression action with a PDMS gasket (~300 μm). Pyrex satisfies several criteria for the substrate, including thermal stability at the process temperature (~95 °C), resistance to process chemicals, optical transparency, and high electrical resistivity. Similarly, SU8 is effective as the microchannel material because of its chemical, and thermal stability, and because it is readily fabricated with vertical sidewalls and high aspect ratios,³⁰ properties which have led to its widespread and

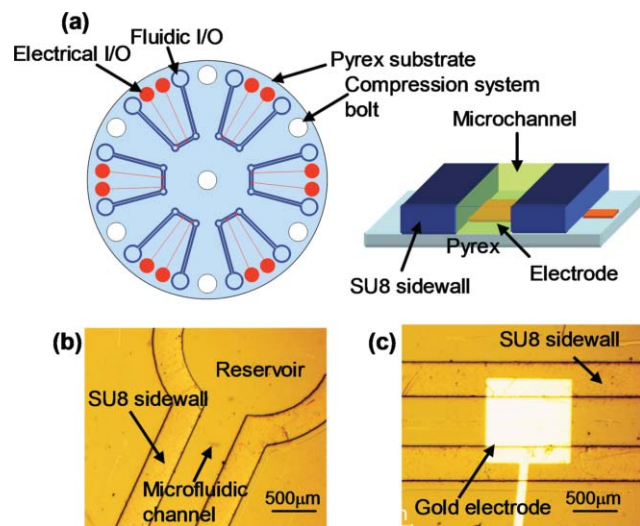


Fig. 2 (a) Design of the microfluidic device wafer and 3-D view of test site; (b) optical microscopy image of the SU8 and microfluidic channel; (c) magnified image of patterned gold (1 mm × 1 mm) underneath the SU8 microfluidic channel.

increasing use as a photoimageable dielectric in lithography for MEMS (microelectromechanical systems) and microfluidics applications. In addition, because SU8 has a higher refractive index than that of both Pyrex and PDMS, it can be used as an optical waveguide when integrated into the SU8 patterns of the microfluidic device wafer, enabling another means for real-time, *in situ* optical analysis of biomolecule assembly in the microfluidic device.²³ This represents an extension of the goal in this work, where our device and packaging design was chosen to enable optical imaging through transparent layers from the top.

Nonpermanent device packaging and leak-free sealing

Fig. 3(a) shows a schematic view of the device packaging process to achieve nonpermanent, consistently leak free sealing. First, the PDMS-spun top sealing plate is placed on top of the microfluidic device. Additional top and bottom Plexiglas plates as well as a top Plexiglas ring with fluidic and electrical ports are then placed and sealed with pressure-adjustable compression bolts at the center and the periphery, and additional set screws, as shown in Fig. 3(c). The completed device, as shown in Fig. 3(c), has microtubing for fluid transport and electrical input/output connections for signal-guided biomolecule assembly connected to the device. A close-up view of one of the microfluidic channels (Fig. 3(d)) with

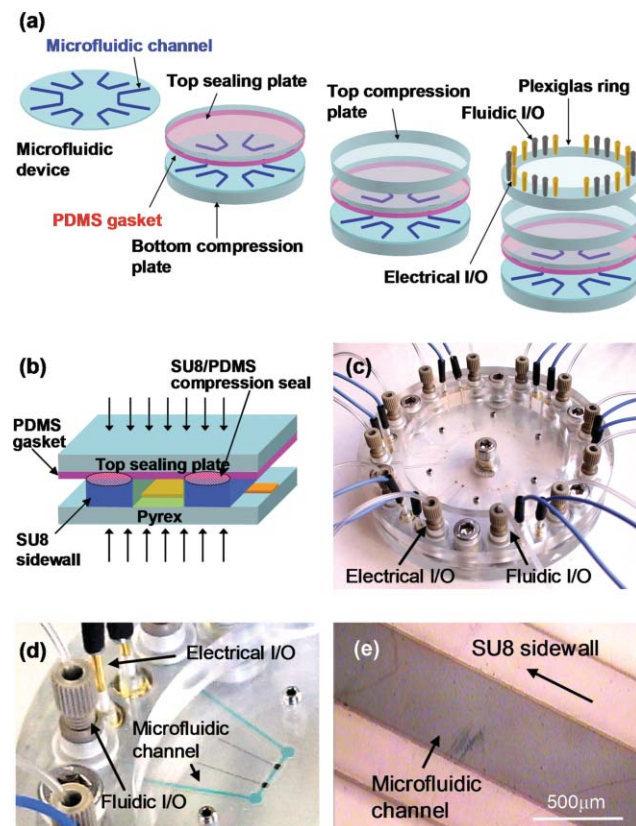


Fig. 3 (a) Schematic view of the microfluidic device packaging process; (b) schematic view of microfluidic sealing; (c) Plexiglas microfluidic package for the microfluidic device wafer; (d) magnified image of the microfluidic system with blue dye solution inside the channel; (e) microscope image of fluid inside the channel.

blue dye solution in the channel shows (1) well-defined channel structure, (2) two gold electrode sites at the bottom of the channel and connected to the I/O port, (3) all-transparent materials for *in situ* optical examination and (4) leak-free sealing, also shown in Fig. 3(e). As shown in the schematic diagram of Fig. 3(b), the consistent leak-free sealing of the microfluidic channel is achieved by partial deformation of the thin, flexible PDMS layer spun onto the top sealing plate through compression bolts with well-controlled pressure. Importantly, repeated disassembly/assembly of the packaged device with leak tests using the dye solution showed consistent leak-free sealing with no sign of deterioration, suggesting the robustness of our sealing strategy.

Chitosan electrodeposition in microfluidic channels at readily addressable assembly sites

As shown in Fig. 4, we demonstrate programmed assembly of biological materials in the microfluidic system through electrodeposition of fluorescently labeled chitosan biopolymer film at a readily addressable electrode site in a microchannel upon completion of the device packaging. Electrolysis of water generates a high pH region on the negatively biased gold electrode surface, which together with the electric field at the surface leads to chitosan layer deposition at this electrode site.^{19,20} As indicated in the schematic drawing in Fig. 4(a), the chitosan molecules are protonated in the low-pH bulk solution, but become deprotonated as they enter the high pH region near the negative electrode and form a biopolymeric hydrogel network at the electrode surface with high spatial resolution.²⁰

First, fluorescently labeled chitosan solution was introduced into the microfluidic channel using a micropump. After the fluidic channel was filled with the solution, the pump was stopped and negative bias (relative to another electrode in the system) was applied to the assembly electrode. The chitosan solution was then drained off and the channel was rinsed with distilled water. As shown in the fluorescence micrograph of

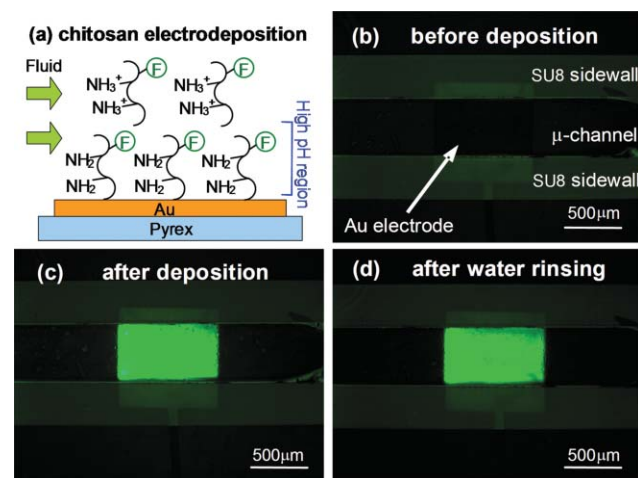


Fig. 4 (a) Schematic drawing of chitosan electrodeposition at the negatively biased electrode in the microfluidic channel; (b–d) fluorescence micrographs of the assembly site in microchannel (b) before deposition, (c) after deposition, (d) after final water rinsing. Chitosan deposition was carried out at 2 A m^{-2} for 240 s.

Fig. 4(b), no significant fluorescence is observed before the chitosan electrodeposition. Upon the electrodeposition of chitosan, Fig. 4(c) shows significant fluorescence well confined in the electrode region, illustrating the presence of assembled chitosan layer. Importantly, the assembled chitosan layer was well retained through rinsing procedure, as shown in Fig. 4(d). This result indicates that biopolymer chitosan can be assembled at readily addressable sites from the aqueous solution through an electric signal. These results also illustrate that biopolymeric material (in this case chitosan) can be assembled in the microfluidic channel after completion of the device fabrication and packaging, and that our nonpermanent packaging strategy for transparent devices allows *in situ* examination of the biomolecular assembly sites through fluorescence microscopy.

Fluorescent labeling of electrodeposited chitosan

As shown in Fig. 5, we then demonstrate conjugation of a fluorescent marker to the electrodeposited chitosan, and

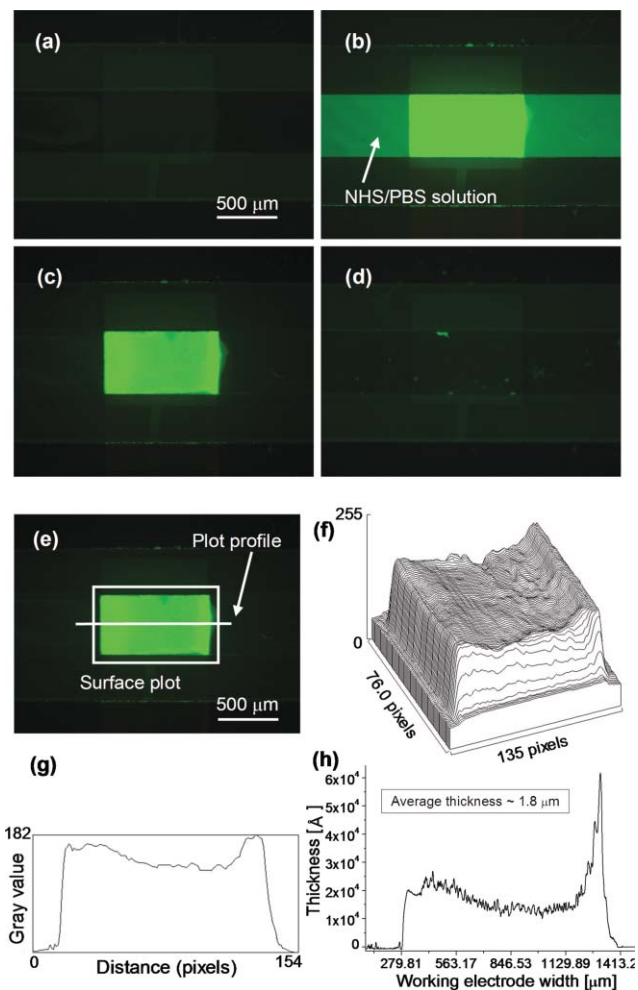


Fig. 5 (a) After chitosan deposition; (b) NHS-fluorescein solution filled in the microfluidic channel; (c) after labeling reaction; (d) negative control channel (no bias); (e) fluorescently labeled chitosan film showing the areas/sections for fluorescence profile analyses; (f) Image J surface plot; (g) Image J plot profile; (h) thickness by mechanical profilometry.

further analyze the assembled layer by comparing the fluorescence intensity profile and physical thickness. First, unlabeled chitosan was electrodeposited at the assembly site by introducing chitosan solution into the microchannel and applying negative bias. As shown in Fig. 5(a), the unlabeled chitosan yields no significant fluorescence upon electrodeposition. As shown in Fig. 5(b), amine group-reactive NHS-fluorescein solution was then introduced into the microchannel. NHS-fluorescein selectively reacts with chitosan's abundant amine groups to form covalent amide linkage, resulting in fluorescent labeling of chitosan.^{19,20} Fig. 5(c) shows that only the assembly site was fluorescently labeled, demonstrating the retained chemical reactivity and spatial selectivity of the electrodeposited chitosan layer. This result strongly suggests that electrodeposited chitosan layer can serve as a spatially selective scaffold for post-fabrication, *in situ* covalent conjugation of biological molecules. To confirm that the chitosan is required for such conjugation, we then performed an identical sequence of events in a separate microchannel, except that the negative bias was not applied to the electrode. As shown in Fig. 5(d), the assembly site showed no noticeable fluorescence upon the introduction of chitosan without negative bias and then NHS-fluorescein, confirming that the fluorescence shown in Fig. 5(c) indeed resulted from conjugation of fluorescein to the electrodeposited chitosan. Next, we analyzed the fluorescence intensity of the labeled chitosan using ImageJ image analysis software and Fig. 5(e) shows the areas/sections for fluorescence profile analyses. As shown in Fig. 5(f). This 3-D contour profile shows relatively uniform fluorescence along the length of the assembly site with slightly higher intensity around the electrode edges. Finally, we examined the chitosan layer by disassembling the nonpermanently sealed package and by measuring the thickness using a mechanical profilometer. As shown in Fig. 5(h), the actual thickness profile showed good agreement with the fluorescence profile (Fig. 5(g)), indicating that the fluorescence profile obtained by *in situ* fluorescence labeling and observation reflected the actual amount of chitosan well. Importantly, this result illustrates that our nonpermanent sealing scheme enables simple *ex situ* examination of physical properties that reaffirms the results obtained by *in situ* optical examination of the assembly and conjugation of biomolecular layer. Combined, these results show that electrodeposition of chitosan enables further post-fabrication, *in situ* biomolecular assembly by harnessing the abundant amine groups of chitosan that retained chemical reactivity upon electrodeposition.

Post-fabrication *in situ* protein assembly onto electrodeposited chitosan scaffold in the microfluidic channels

Finally, we demonstrate *in situ* protein assembly onto electrodeposited chitosan scaffold through a chemical cross-linking reagent in the microfluidic channel, as shown in Fig. 6. For this, we reassembled the microfluidic device after the profilometer measurement (Fig. 5(h)), and electrodeposited chitosan at a separate microfluidic channel on the same wafer. Then we introduced 0.5% aqueous solution of glutaraldehyde, an amine group reactive homobifunctional crosslinker that

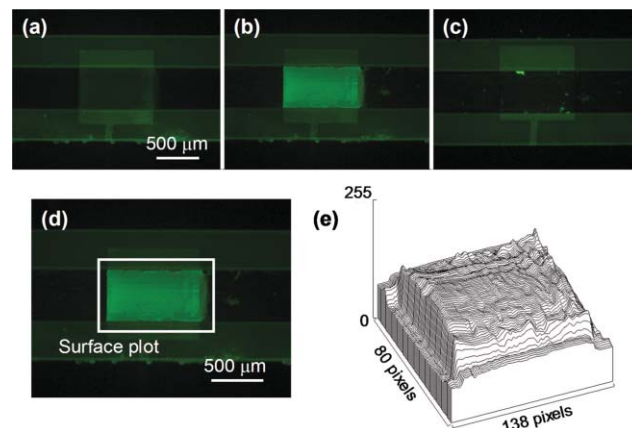


Fig. 6 (a) Fluorescence image of the assembly site after glutaraldehyde reaction; (b) after GFP reaction; (c) negative control (no bias); (d) GFP conjugated chitosan film; (e) Image J fluorescence surface plot.

activates chitosan for covalent coupling with amine groups on proteins. As shown in Fig. 6(a), no significant fluorescence appears up to this activation step as expected. Next, we introduce aqueous solution of green fluorescent protein (GFP) into the microchannel. Fig. 6(b) illustrates that GFP reacts with and becomes conjugated onto the activated chitosan scaffold. This result shows that electrodeposited chitosan enables post-fabrication, *in situ* assembly of proteins in microfluidic channels through a series of simple standard chemical reactions all in an aqueous environment. Importantly, the assembled GFP retains the fluorescence (Fig. 6(b)), indicating that the structure of the protein is preserved throughout the assembly procedure. In contrast, Fig. 6(c) shows a negative control channel, which underwent the identical procedure as the previous channel (Fig. 6(b)) except that the electrode was not negatively biased for chitosan electrodeposition. This result reconfirms that the *in situ* protein assembly requires electrodeposited chitosan as the covalent coupling scaffold. Further, fluorescence profile analysis was performed on the assembly site (Fig. 6(d)) and the 3-D fluorescent contour shows uniform fluorescence intensity of the GFP decorated chitosan film (Fig. 6(e)). Combined, these results demonstrate *in situ* protein assembly in the microfluidic device, which could be further exploited for biochemical reactions or biosensing applications based on *in situ* assembled enzymes or antibodies at readily addressable, activated chitosan scaffold sites in microfluidic devices. Particularly important to note is that the sequences of steps and electric signal-guided biomolecule assembly strategy allow an all-aqueous environment for the protein assembly, preserving the biological activities.

Conclusions

This paper demonstrates post-fabrication biomolecule assembly at readily addressable sites inside the microfluidic channel after the device is completely packaged. For this, we developed a microfluidic device with several unique features. First, all transparent materials allow simple *in situ* observation of the assembly processes by an optical and/or fluorescence microscope. Second, nonpermanent packaging by flexible

PDMS-spun on the top sealing plate and compression bolts ensure consistent leak tight sealing as well as convenient *ex situ* analysis. Third, micropatterned gold electrodes at the bottom of the microfluidic channel provide readily addressable, signal-guided biomolecule assembly sites. Finally, fluidic and electrical input/output ports provide fluid transport and electrical signal for the biomolecule assembly.

Harnessing this microfluidic device we subsequently demonstrated spatially selective assembly of the device–biology interface chitosan by taking advantage of its pH-responsive property. We then demonstrated transport and covalent conjugation of marker molecule fluorescein and GFP onto the electrodeposited chitosan scaffold by taking advantage of its chemical reactivity. The results shown in Fig. 5 and Fig. 6 confirm the retained chemical reactivity of the electrodeposited chitosan scaffold. Importantly, the electrodeposited chitosan was well retained throughout various transport and rinsing procedures, confirming its potential for biomolecule assembly scaffold for future applications. Further, the assembled GFP retained its fluorescence, suggesting that its structure remained intact through the assembly processes.

We believe that our approach for biomolecule assembly in microfluidic devices offer several unique capabilities. First, the electric signal-guided nature of the chitosan assembly allows simple *in situ* assembly of biological molecules when and where it is needed, even long after the device is fully manufactured. This capability may allow biological components to be assembled into complex microfluidic networks (*e.g.* for high throughput drug screening) with greater ease than conventional assembly methods. Second, biomolecules are assembled from the aqueous environment, thus preserving their biological activities through the assembly procedure. Third, our approach is user friendly since the end-user, namely a biologist or a clinician, does not need complex robotic printing facilities or arduous chemical procedures to achieve selective biomolecule assembly. Finally, our technique may offer generic, flexible strategies for different target biomolecules since a wide variety of conjugation schemes can be utilized for different biomolecules.²²

Acknowledgements

This work was supported in part by the NSF under the MRSEC program and the IMI program and by the Laboratory for Physical Sciences. The authors would like to thank Sheng Li for his generous help in using the cleanroom facility in MEMS Sensors and Actuators Lab (MSAL) at the University of Maryland in College Park.

References

- 1 D. J. Beebe, G. A. Mensing and G. M. Walker, *Annu. Rev. Biomed. Eng.*, 2002, **4**, 261.
- 2 A. Hiratsuka, H. Muguruma, K. H. Lee and I. Karube, *Biosens. Bioelectron.*, 2004, **19**, 1667.
- 3 C. H. Ahn, J. W. Choi, G. Beaucage, J. H. Nevin, J. B. Lee, A. Puntambekar and J. Y. Lee, *Proc. IEEE*, 2004, **92**, 154.
- 4 D. Kim and M. L. Shuler, *Proc. SPIE–Int. Soc. Opt. Eng.*, 2004, **5321**, 309.
- 5 T. Fujii, *Microelectron. Eng.*, 2002, **61–2**, 907.
- 6 H. Becker and L. E. Locascio, *Talanta*, 2002, **56**, 267.
- 7 J. W. Choi, K. W. Oh, J. H. Thomas, W. R. Heineman, H. B. Halsall, J. H. Nevin, A. J. Helmicki, H. T. Henderson and C. H. Ahn, *Lab Chip*, 2002, **2**, 27.
- 8 D. J. Harrison, K. Fluri, K. Seiler, Z. H. Fan, C. S. Effenhauser and A. Manz, *Science*, 1993, **261**, 895.
- 9 L. Bousse and W. Parce, *IEEE Eng. Med. Biol. Mag.*, 1994, **13**, 396.
- 10 G. J. M. Bruin, *Electrophoresis*, 2000, **21**, 3931.
- 11 G. H. W. Sanders and A. Manz, *Trends Anal. Chem.*, 2000, **19**, 364.
- 12 J. Liu, C. Hansen and S. R. Quake, *Anal. Chem.*, 2003, **75**, 4718.
- 13 S. P. A. Fodor, J. L. Read, M. C. Pirrung, L. Stryer, A. T. Lu and D. Solas, *Science*, 1991, **251**, 767.
- 14 Y. N. Xia and G. M. Whitesides, *Annu. Rev. Mater. Sci.*, 1998, **28**, 153.
- 15 S. A. Lange, V. Benes, D. P. Kern, J. K. H. Horber and A. Bernard, *Anal. Chem.*, 2004, **76**, 1641.
- 16 A. P. Blanchard, R. J. Kaiser and L. E. Hood, *Biosens. Bioelectron.*, 1996, **11**, 687.
- 17 C. D. Bain, E. B. Troughton, Y. T. Tao, J. Evall, G. M. Whitesides and R. G. Nuzzo, *J. Am. Chem. Soc.*, 1989, **111**, 321.
- 18 H. M. Yi, L. Q. Wu, W. E. Bentley, R. Ghodssi, G. W. Rubloff, J. N. Culver and G. F. Payne, *Biomacromolecules*, 2005, **6**, 2881.
- 19 L. Q. Wu, A. P. Gadre, H. M. Yi, M. J. Kastantin, G. W. Rubloff, W. E. Bentley, G. F. Payne and R. Ghodssi, *Langmuir*, 2002, **18**, 8620.
- 20 L. Q. Wu, H. M. Yi, S. Li, G. W. Rubloff, W. E. Bentley, R. Ghodssi and G. F. Payne, *Langmuir*, 2003, **19**, 519.
- 21 H. M. Yi, L. Q. Wu, R. Ghodssi, G. W. Rubloff, G. F. Payne and W. E. Bentley, *Anal. Chem.*, 2004, **76**, 365.
- 22 H. M. Yi, L. Q. Wu, R. Ghodssi, G. W. Rubloff, G. F. Payne and W. E. Bentley, *Langmuir*, 2005, **21**, 2104.
- 23 M. A. Powers, S. T. Koev, A. Schleunitz, H. M. Yi, V. Hodzic, W. E. Bentley, G. F. Payne, G. W. Rubloff and R. Ghodssi, *Lab Chip*, 2005, **5**, 583.
- 24 W. Tan and T. A. Desai, *Biomed. Microdev.*, 2003, **5**, 235.
- 25 Z. L. Zhang, C. Crozatier, M. Le Berre and Y. Chen, *Microelectron. Eng.*, 2005, **78–79**, 556.
- 26 X. G. Li, T. Abe, Y. X. Liu and M. Esashi, *J. Microelectromech. Syst.*, 2002, **11**, 625.
- 27 K. R. Williams, K. Gupta and M. Wasilik, *J. Microelectromech. Syst.*, 2003, **12**, 761.
- 28 B. Keiper, H. Exner, U. Loschner and T. Kuntze, *J. Laser Appl.*, 2000, **12**, 189.
- 29 S. D. Senturia, *Microsystem Design*, Kluwer Academic Publishers, Massachusetts, 2002, ch. 3, pp. 50–54.
- 30 J. Carlier, S. Arscott, V. Thomy, J. C. Fourier, F. Caron, J. C. Camart, C. Druon and P. Tabourier, *J. Micromech. Microeng.*, 2004, **14**, 619.